Modeling the Concentric Organization of Lattices and Path-Regular Networks and Its Application to Complex Neuronal Networks Analysis

Luciano da Fontoura Costa
Institute of Physics at São Carlos, University of São Paulo,
PO Box 369, São Carlos, São Paulo, 13560-970 Brazil
(Dated: 21st Feb 2008)

The concentric organization of a complex network with respect to a reference node can provide rich information about both the topology and the dynamics of complex networks. Particularly, measurements such as the hierarchical number of nodes, the hierarchical degree and the intra-ring degree have been recently shown (arXiv:0802.0421 and arXiv:0802.1272) to define important features of non-linear dynamics taking place in complex networks. The current article reports theoretical models capable of reproducing with high accuracy the concentric organization, expressed in terms of the three just-mentioned measurements, of two important types of networks, namely orthogonal lattices and path-regular structures. The potential of such models is illustrated with respect to their application to systematic characterization of non-linear integrate-and-fire dynamics in those two types of networks, more specifically the prediction of avalanches of spikes and their properties.

PACS numbers: 87.18.Sn, 05.40Fb, 89.70.Hj, 89.75.Hc, 89.75.Kd

'This is the foundation of the city: a net which serves as passage and as support.' (Invisible Cities, I. Calvino)

I. INTRODUCTION

Given a complex network (e.g. [1–5]), its structural properties can be quantified and analysed by taking several measurements and investigating their specific distributions and relationships [5]. In case the network underlies specific types of dynamics, the obtained measurements can also be related to specific dynamical features, an approach which underlies the so-called structure-dynamics paradigm (e.g. [3, 4]).

Though complex networks can be characterized while taking into account statistics (e.g. mean and standard deviation) of the considered measurements, defining the *global* analysis approach [5], it is often important to resort also to local structural or dynamical features. Two main approaches are possible: node- and edge-based. For instance, in the former case, the consideration of the individual node degrees or clustering coefficients can allow the identification of deviating connectivity patterns, such as hubs (see also [6]). Many are the node-based measurements which have been proposed and used for the characterization and classification of complex networks (e.g. [5]). Edge-based measurements are much less common. Interestingly, edge-based measurements can be immediately obtained by the line graph method of transforming complex networks (e.g. [7, 8]) and taking the traditional node-based measurements, but this approach has also been rarely applied.

One node-based family of measurements, called *hierarchical* or *concentric* (e.g. [9–12]), is particularly interesting because it allows the characterization of the connectivity surrounding each node in terms of a progressive range of topological scales, giving rise to a *multiscale* approach. More specifically, given a network Γ and one of its nodes i, a series of *concentric levels* or rings can be defined corresponding to the set $C_1(i)$ of immediate neighbors of node i (level 1), the set $C_2(i)$ of the immediate neighbors of $C_1(i)$, and so forth until the network is completely covered. Once such concentric levels have been determined, it becomes possible to obtain a whole series of hierarchical measurements [9–12], including the hierarchical number of nodes, the hierarchical degree and the intra-ring degree at each level h. The *hierarchical number of nodes* at level h of a network with respect to a given reference node corresponds to the number of elements in the set $C_h(i)$. The *hierarchical degree* at level h of a node i has been defined [9] as the number of edges extending between levels h and $h+1$ (this concept can be immediately extended to directed networks). The *intra-ring degree* at level h of a node i is the number of edges connecting pairs of nodes within level h. The potential of such measurements, as well as of additional concentric features, has been illustrated with respect to several theoretical and real-world investigations (e.g. [9–12]).

More recently [13–15], it was shown that important types of non-linear dynamics, such as integrate-and-fire (e.g. [16]) neuronal activation in presence of facilitation (e.g. [17]), are intrinsically underlain by the concentric organization of the respective networks. More specifically, it has been shown [13] that the important dynamical phenomena of avalanches of activation [15] and activation confinement within communities [14, 18] are intrinsically defined by the hierarchical number of nodes, hierarchical degrees and intra-ring degrees. Such a finding motivated the introduction of *equivalent models* of the structure of the network under analysis, allowing the estimation of important dynamical features while considering only a handful of equivalent nodes, which were enough to capture the intrinsic dynamical features underlying the non-linear phenomena of avalanches and activation confine-

ment.

Such results motivate further attention to be given to the concentric organization of complex networks. Because important structural and dynamical properties of the network under analysis are ultimately related to its hierarchical number of nodes, hierarchical degrees and intra-ring degrees, it would be particularly interesting to develop theoretical models of the concentric organization of specific types of complex networks which could allow systematic analytical investigations of the structure and dynamics of networks without resorting to computational simulations involving several realizations of each network type. This represents precisely to the main objective of the current work. More specifically, we develop analytical models of the hierarchical organization — expressed in terms of the hierarchical number of nodes, hierarchical degrees and intra-ring degrees — for two particularly relevant theoretical models of complex networks, namely orthogonal lattices and the path-regular complex networks introduced recently as a member of the larger family of knitted networks [19, 20].

Though ubiquitous in traditional dynamical systems, regular lattices such as orthogonal and hexagonal grids have rarely been considered in complex network research. Yet, these networks are particularly important because they exhibit completely regular node degrees. In addition, they are completely deterministic instead of stochastic (such as Erdős-Rényi networks). In this work we restrict our attention to thoroidal (periodic) orthogonal grids with degree 4. The other type of complex network model considered here, namely the path-regular networks, has been introduced recently [19, 20] as a special type of knitted network. Basically, a path regular network, henceforth abbreviated as PN, is obtained by starting with N isolated nodes and performing M paths encompassing all these nodes (recall that a path never repeats a node or an edge). As a consequence most nodes exhibit identical degrees equal to $2M$ (i.e. each path contributes with 2 edges for each node). In addition to being intrinsically related to the somewhat overlooked path-organization of networks, PN structures have been found (e.g. [20–22]) to yield particularly uniform values of almost every possible measurements, not only between nodes but also between different realizations with the same size and average degree. PN networks are also natural candidates for modeling real-world structures underlain by paths, such as neuronal networks, as well as transportation and communication systems. The PN model was later modified [13] in order to obtain all nodes with identical degrees. This can be easily achieved by connecting the extremities of each of the M paths and not allowing a path to go through an edge belonging to a previous path. This type of network, henceforth abbreviated as PI, is considered henceforth in this article.

In order to illustrate the potential of the analytical models reported in this work, we apply them to the characterization, through the respective equivalent models, of avalanches of spikes in of integrate-and-fire complex neuronal networks. Two types of dynamics are considered, involving the distribution of the axon activation as well as the more biologically-realistic situation of fixed action potentials. In both cases, respective criteria are presented allowing the prediction of the strength of the avalanches.

This work is organized as follows. It starts by briefly reviewing the basic concepts in complex network concentric characterization, as well as introducing the regular lattices and path-regular networks, and proceeds by developing the analytical models of the regular lattices and path-regular networks and showing the adherence of the predictions obtained by using such models against real measurements obtained by considering ensembles of whole networks. The potential of the developed models is then illustrated with respect to the study of avalanches in lattice and path-regular complex neuronal networks with integrate-and-fire dynamics.

II. CONCENTRIC CHARACTERIZATION OF COMPLEX NETWORKS: BASIC CONCEPTS

A complex undirected and unweighted network Γ can be completely represented in terms of its *adjacency matrix* K, of dimension $N \times N$. Each edge between two nodes i and j, $i, j \in \{1, 2, \ldots N\}$, implies $K(j,i) = K(i,j) = 1$. The absence of connection between those to nodes is expressed as $K(j,i) = K(i,j) = 1$. Two nodes are *adjacent* whenever they share an edge. Two edges are adjacent if they share a node. A sequence of adjacent edges is a *walk*. A walk which never repeats a node or edge is called a *path*. Given a node i, the nodes which are adjacent to it are henceforth called its *immediate neighbors*. The set of immediate neighbors of a node i is abbreviated as $C_1(i)$; the set of immediate neighbors of the nodes in $C_1(i)$ defines the new set $C_2(i)$, and so on. The set $C_h(i)$ is herein called the *concentric (or hierarchical) level (or ring)* of the network Γ with respect to the reference node i. The whole set of concentric levels, from $h = 0$ (i.e. the original node i) up to a maximum level H is called the *hierarchical organization* of the complex network γ with respect to node i. The number of nodes in $C_h(i)$ (i.e. the cardinality of this set, herein represented as $|C_h(i)|$) is called the *hierarchical number of nodes* at level h with respect to i. The number of edges extending between the concentric levels h and $h+1$ is called the *hierarchical degree* of node i at level h. The number of edges connecting pairs of nodes inside a given level h is the *intra-ring degree* of node i at level h. An example of a network and respective hierarchical measurements can be found in Section IV, Figures 1 and Figures 2.

III. ORTHOGONAL LATTICES AND THE PATH-REGULAR NETWORKS

In an infinte *orthogonal lattice*, each node is connected to its four adjacent neighbors. A finite orthogonal lattice with periodic (or thoroidal) boundary conditions of dimension $L \times L$ includes a total of $N = L^2$ nodes and $E = 2N$ edges. The average degree therefore is given as $\langle k \rangle = 2E/N = 4$, with null standard deviation, implying all nodes to have the same degree. Figure 1 depicts a 5×5 finite orthogonal lattice with periodic boundary conditions.

The *knitted* family of complex networks was introduced recently [19, 20] in order to represent networks defined by *paths*, instead of star connectivity. Two main types of such networks have been proposed so far: path-transformed BA networks (PA) and path-regular networks (PN). The former is obtained by path-star transforming BA networks, so that the edges in each star is transformed into a respective path. As a consequence of such a construction procedure, such networks exhibit a scale-free distribution of shortest-path lengths. The second category of knitted networks, namely the path-regular (PN) structures, is substantially simpler and can be obtained as follows: (i) start with N isolated nodes; (ii) perform M path-walks encompassing all nodes. By emphpath walk it is meant a walk where no edge or node are repeated. PN networks have been found to exhibit particularly uniform connectivity, yielding similar values for several measurements taken amongst nodes or amongst different realizations of the same configuration (e.g. [20–22]). More recently [13], a version of the PN networks, henceforth abbreviated as PI, was proposed which is still more uniform than the PN structures. This type of network is obtained by incorporating two additional conditions on the PN generation, namely: (a) the extremities of each of the M path-walks are connected; and (b) the path-walks are not allowed to cover edges or nodes belonging to the previous path-walks. As a consequence of such additional constraints, the PI networks result with all nodes having identical degree equal to $2M$.

It is interesting to make a brief discussion of the possible relationships between the orthogonal lattice and a PI network with the same number of nodes and degree. Though both these structures would be undistinguishable as far as the node degree is concerned (all nodes have degree equal to 4), almost any other possible measurements result quite distinct distributions, reflecting the fact that the node degree provides but a degenerate (incomplete) characterization of the network overall connectivity. One particularly relevant aspect in which the orthogonal lattice and PI networks differ one another concerns the number of paths of several lengths between any two adjacent nodes. It is also interesting to observe that, while the connectivity of orthogonal lattices is deterministic, the connections in a PI (or PN) network are stochastic, yielding diverse structures for different realizations of the same parametric configuration (recall that the PI network has just two parameters, its size N and the number of incorporated path-walks M).

IV. ANALYTICAL MODEL OF THE CONCENTRIC ORGANIZATION OF ORTHOGONAL LATTICES

Because of the orthogonal symmetry of this discrete structure, identical hierarchical organizations are obtained with respect to *any* of its nodes. In this section we develop an analytical expression for the hierarchical number of nodes, hierarchical degree and intra-ring degree of infinite and finite orthogonal lattice of any size $N = L^2$.

We start by considering the infinite case. Starting at any node i, we have $n_0(i) = |C_0(i)| = 1$ nodes; $n_1(i) = |C_1(i)| = 4$ nodes; $n_2(i) = |C_2(i)| = 8$ nodes; $n_3(i) = C_3(i) = 12$; $n_4(i) = |C_4(i)| = 16$; and so on up to the last concentric level H. More generally, it can be shown that $n_h(i) = |C_h(i)| = 4h$. Similarly, we have that $k_h(i) = 2n_h(i) + 4$ and $a_h(i) = 0$ for $h = 0, 1, \ldots, H$.

The case of finite orthogonal lattices is more properly analysed by considering separately the cases in which L is even or odd. In the former situation, i.e. L *even*, the hierarchical number of nodes and hierarchical degrees are symmetric with respect to $h = \lfloor L/2 \rfloor$, while the intra-ring degrees are all zero. More specifically, in the case of finite orthogonal lattices with L even, we have

$$n_h(i) = \begin{cases} 1 & \text{if } h = 0 \\ 4h & \text{if } h = 1, 2, \ldots, \lfloor L/2 \rfloor - 1 \\ n_{H-h}(i) & \text{if } h = \lfloor L/2 \rfloor + 1, \ldots, H \\ 2L - 2 & \text{if } h = \lfloor L/2 \rfloor \end{cases}$$

$$k_h(i) = \begin{cases} 4 & \text{if } h = 0 \\ 2n_h(i) + 4 & \text{if } h = 1, 2, \ldots, \lfloor L/2 \rfloor - 1 \\ k_{H-h-1}(i) & \text{if } h = \lfloor L/2 \rfloor, \ldots, H - 1 \\ 0 & \text{if } h = H \end{cases}$$

$$a_h(i) = 0, \text{for any } h$$

The finite orthogonal lattice for L *odd* yields a somewhat more complex situation. Though the hierarchical number of nodes is still symmetric with respect to $h = \lfloor L/2 \rfloor$, the hierarchical degrees are not, while the intra-ring degrees are no longer null. Figure 1 illustrates the periodic orthogonal lattice with dimension 5×5 (a) and its respective concentric organization (b).

Figure 2 shows the hierarchical number of nodes $k_h(i)$, the hierarchical degrees $k_h(i)$, and the intra-ring degrees $k_h(i)$ of the finite 5×5 orthogonal lattice in Figure 1.

Interestingly, the intra-ring degrees are no longer zero, but increase towards a plateau equal to 4 for $h \geq \lfloor L2 \rfloor$. The hierarchical number of nodes, hierarchical degrees

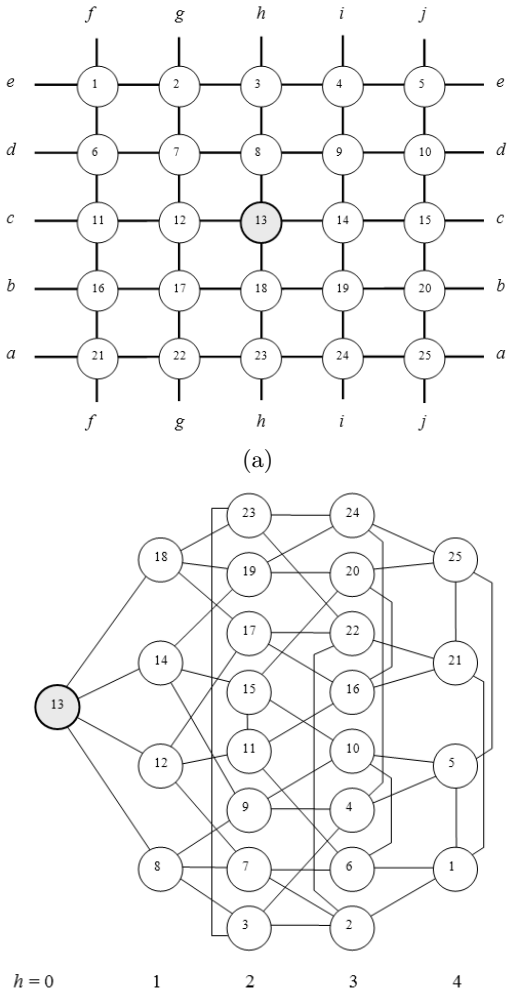

FIG. 1: The 5 orthogonal lattice (a) and its respective concentric (or hierarchical) organization (b) involving 5 levels.

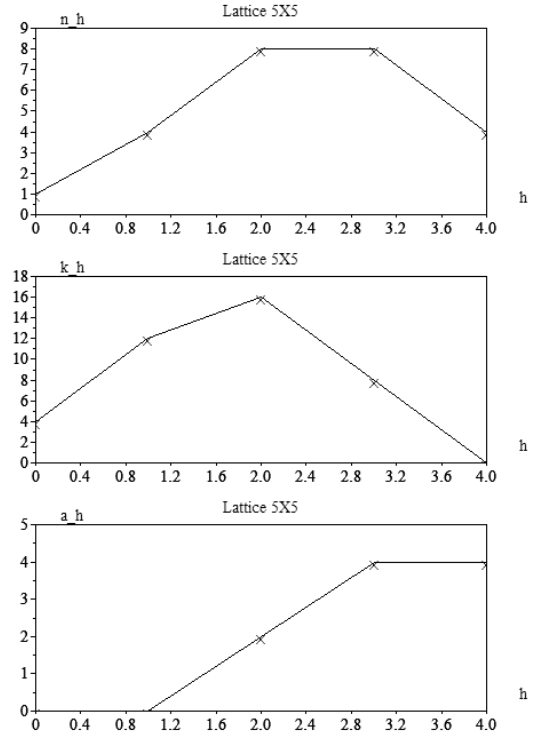

FIG. 2: The hierarchical number of nodes $n_h(i)$, the hierarchical degree $k_h(i)$ and the intra-ring degree $a_h(i)$, with respect to node 13, of the orthogonal lattice in Fig. 1.

and intra-ring degrees of a finite thoroidal lattice with L odd can be calculated as follows

$$n_h(i) = \begin{cases} 1 & \text{if } h = 0 \\ 4h & \text{if } h = 1, 2, \ldots, \lfloor L/2 \rfloor - 1 \\ n_{H-h+1}(i) & \text{if } h = \lfloor L/2 \rfloor + 1, \ldots, H \\ 2L - 2 & \text{if } h = \lfloor L/2 \rfloor \end{cases}$$

$$k_h(i) = \begin{cases} 4 & \text{if } h = 0 \\ 2n_h(i) + 4 & \text{if } h = 1, 2, \ldots, \lfloor L/2 \rfloor - 1 \\ k_{H-h-1}(i) + 4 & \text{if } h = \lfloor L/2 \rfloor, \ldots, H - 1 \\ 0 & \text{if } h = H \end{cases}$$

$$a_h(i) = \begin{cases} 0 & \text{if } h = 0, 1, \ldots, \lfloor L/2 \rfloor - 1 \\ 2 & \text{if } h = \lfloor L/2 \rfloor \\ 4 & \text{if } h = \lfloor L/2 \rfloor + 1, \ldots, H \end{cases}$$

V. ANALYTICAL MODEL OF THE CONCENTRIC ORGANIZATION OF PATH-REGULAR NETWORKS

Because of stochastic symmetry, similar concentric organizations are obtained for a PI network considering any of its nodes as reference. In order to obtain an analytical

model of the concentric organization of the PI networks, we start by developing a recursive mean field formulation taking into account the concentric organization with respect to any node i. Henceforth, we represent the average degree of the PI network as $\langle k \rangle$ and, because similar results are obtained for any reference node i, we omit the reference node identification (e.g. $n_h(i)$ becomes n_h).

Starting with any of its nodes i, we have $n_0 = 1$; $k_0 = \langle k \rangle$ and $a_0 = 0$. At the next concentric level, one node will be found attached to each of the edges emanating from the reference node i, so that $n_1 = \langle k \rangle$. Now, each of these $\langle k \rangle$ nodes in the first concentric level $h = 1$ of the network will have $\langle k \rangle - 1$ free edges (recall that one of the edges was already used to connect to i). These $\langle k \rangle - 1$ edges can be used to implement intra-ring connections within $h = 1$ or for connecting to the subsequent level $h = 2$. Let us represent the remainder of nodes not yet used while at a level h as R_h, so that $R_1 = N - \langle k \rangle - 1$ (i.e. the total of nodes minus the reference node and the $\langle k \rangle$ nodes belonging to $h = 1$). Each of the available $k - 1$ edges of each of the $\langle k \rangle$ nodes at $h = 1$ will have a probability of staying inside that level given as $p_h = n_h/R_{h-1} = n_h/(R_h + n_h)$. Therefore, the intra-ring degree of level h can be estimated as being equal to $a_h = 0.5 \langle k \rangle * (\langle k \rangle - 1) * p_h$, leaving a total of $k_h = \langle k \rangle * (k-1) * (1-p_h)$ edges for implementing connections with the next hierarchical level.

Unlike the situation from level $h = 0$ to 1, the number of nodes which will be incorporated into level $h = 2$ is not equal to the number of edges between levels $h = 1$ and $h = 2$ (i.e. the hierarchical degree k_1) because more than one of such edges may connect to a same node at the next layer $h = 2$. The number of nodes which will be incorporated into level $h = 2$ can be estimated as being equal to $n_2 = \eta(n_1, E_1, R_1)$, where $\eta()$ is the function defined below and $E_h = k_h/n_h$.

$$\eta(n_h, E_h, R_h) =$$

$$= \begin{cases} R_h & \text{if } R_h \leq E_h \\ R_h \left[1 - \left(1 - \frac{E_h}{R_h}\right)^{n_h}\right] & \text{if } R_h > E_h \end{cases}$$

This function is obtained by considering that the first of the n_h nodes at level h will connect to E_h nodes, the second of the nodes at level h will connect to $(R_h - E_h)/R_h$ nodes, and so forth.

The above basic reasoning can now be extended with respect to level $h = 2$, and so on, until all the N nodes are incorporated into the network. Therefore, the complete procedure for obtaining the concentric organization in terms of the hierarchical number of nodes, hierarchical degree and intra-ring degree, is given as follows

$n_0 = 1$; $a_0 = 0$; $R_0 = N - 1$; $k_0 = \langle k \rangle$; $E_0 = \langle k \rangle$;
$h = 1$;
while $n_{h-1} > 0$ **and** $R_{h-1} > 0$
  $n_h = \eta(n_{h-1}, E_{h-1}, R_{h-1})$;
  $R_h = R_{h-1} - n_h$;
  if $R_h > 0$
    $a_h = 0.5(\langle k \rangle n_h - k_{h-1}) n_h / R_{h-1}$;
    $k_h = (\langle k \rangle n_h - k_{h-1}) R_h / R_{h-1}$;
    if $n_h > 0$
      $E_h = k_h / n_h$;
    end
  end
  $h = h + 1$;
end

The above algorithm has been verified to be capable of reproducing with impressive accuracy the hierarchical number of nodes, hierarchical degrees and intra-ring degrees of PI networks. Figure 3 illustrates the predicted and actual (averaged over 500 realizations) values of these three measurements with respect to PI networks of different size and average degree.

VI. APPLICATION EXAMPLE: ANALYTICAL INVESTIGATION OF INTEGRATE-AND-FIRE AVALANCHES

Complex neuronal networks with integrate-and-fire dynamics have been found [13, 15] to exhibit avalanches of spikes under specific circumstances (e.g. type of network, size, average degree). Interestingly, such a critical phenomenon has bee explained [13] as a consequence of the concentric organization of the respective networks. More specifically, given any network, it is possible to obtain its *equivalent model* by estimating the hierarchical number of nodes, hierarchical degrees and intra-ring degrees. Once such measurements are obtained, the equivalent model is immediately given as shown in Figure 4, i.e. each equivalent node represents the respective $n_h(i)$ original nodes (these values are taken as the threshold of the respective equivalent nodes), the weights of the connections between successive concentric levels correspond to the respective hierarchical degrees $k_h(i)$, while the weights of the self-connections are given by the intra-ring degrees $a_h(i)$.

It has been verified that such a mean-field model yields accurate predictions of the respective dynamics, including avalanches and confinement. In other words, most of the relevant structural features of the original network are captured by the equivalent model, except the inherent variability of degrees between nodes (see also [14], where the equivalent model was enhanced to incorporate groups of nodes with distinct degrees). Therefore, it becomes possible to investigate important dynamical features of complex networks by considering their respective equivalent concentric models. In particular, the analytical models of the concentric organization of the orthogonal lattice and PI networks developed in this article can be immediately applied in order to obtain the respective equivalent models, paving the way for comprehensive investigations of the structure-dynamics relationship.

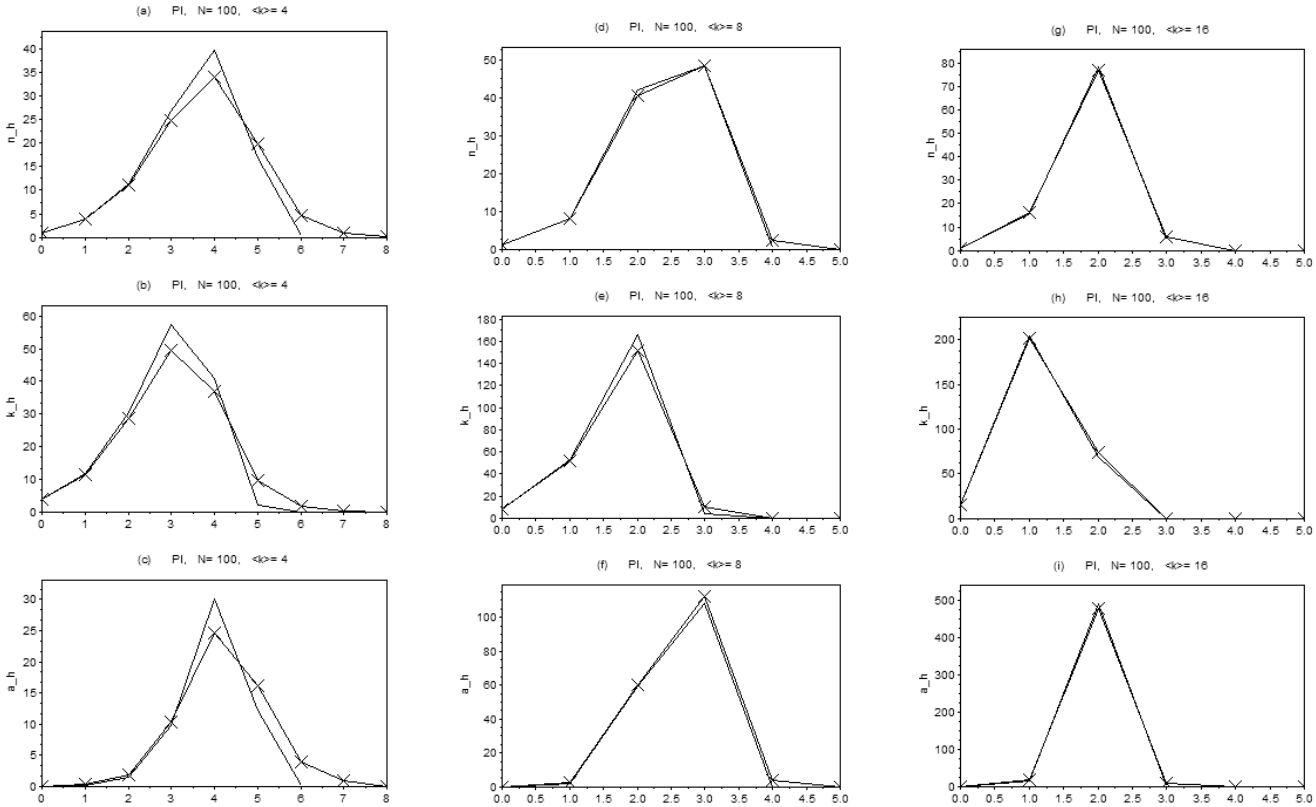

FIG. 3: The predicted and real values (asterisks) of the hierarchical number of nodes $n_h(i)$, the hierarchical degree $k_h(i)$ and the intra-ring degree $a_h(i)$ considering PI networks with several sizes and average degrees.

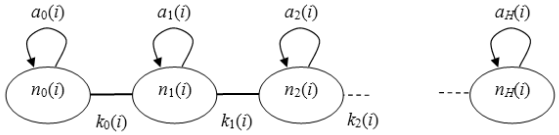

FIG. 4: The equivalent model of a complex network is completely specified by the respective hierarchical number of nodes, hierarchical degrees and intra-ring degrees.

In this section we apply the analytical models of the orthogonal lattice and PI networks in order to investigate in more depth their dynamics regarding the spiking avalanche phenomenon considering two specific situations: (i) *Distributed action potential*, in the sense that, at each spike, the each axon convey a fraction of the internal activation; and (ii) *Fixed action potential*, i.e. each axon conveys spikes with activation 1 (more biologically-realistic). These two situations are addressed in the following respective subsections.

A. Distributed Action Potential

Here we consider that, at each spike, the activation $S(i)$ stored inside each cell i is distributed equally between the outgoing axons. So, once a neuron i associated to a respective node with outdegree $k_{out}(i)$ spikes, each of its $k_{out}(i)$ axons will carry activation equal to $S(i)/k_{out}(i)$. The internal activation is never allowed to exceed its respective threshold $T(i)$. We herein assume identical thresholds $T(i) = T$ for every neuron i.

Because the complex neuronal network is assumed to constitute a connected component, in the sense that any node can be reached from any other node, given enough time all neurons will be activated. However, such an activation can proceed either gradually or abruptly. The latter situation is often characterized by avalanches [13, 15]. The important aspects in the activation of the respective complex neuronal network are the transfer of activation between concentric levels, as well as the portion of activation that remains at each level. For instance, in case the network has several concentric levels with similar number of nodes, it will take longer to activate all levels, and the activation will also be more gradual. In the case of networks involving few concentric levels, it becomes possi-

ble, under specific circumstances, that one or more levels with the largest quantities of nodes are activated almost simultaneously. In these cases, it can be shown that the sharpness and height of the avalanches, are related to the two following ratios:

$$r1(i) = \frac{n_h(i)}{n_{h+1}(i)} \frac{k_h(i)}{k_h(i) + k_{h-1}(i) + a_h(i)} \frac{1}{T}$$
$$r2(i) = \frac{n_h(i)}{n_{h-1}(i)} \frac{k_{h-1}(i)}{k_h(i) + k_{h-1}(i) + a_h(i)} \frac{1}{T}$$

where h refers to the concentric levels containing the largest number of nodes. Ratio $r1$ quantifies the efficiency in which the activation from level h affects the equivalent node in level $h+1$; the ratio $r2$ quantifies such an efficiency with respect to the transfer of activation to the equivalent level $h-1$. Therefore, the larger these ratios, the higher the chances of avalanches (recall that in the equivalent model, the threshold of each equivalent node corresponds to the respective hierarchical number of nodes). In particular, avalanches should be observed for $r1, r2 > 1$. It should be observed that these activation ratios specify not only the chances of avalanches, but also their relative sharpness, in the sense that avalanches obtained for larger ratio values tend to be more abrupt along time. At the same time, sharper avalanches also tend to imply larger amplitudes.

The hierarchical number of nodes, hierarchical degrees and intra-ring degrees of PI networks with different sizes (i.e. $N = 50, 100, 500$ and 1000) and average degrees (i.e. $\langle k \rangle = 46810$ and 12) were obtained by using the respective analytical model developed in Section V, and the ratios $r1$ and $r2$ for the level with the largest number of nodes were calculated as above. Figure 5 shows the obtained scatterplot of $r1 \times r2$. Several interesting features can be observed in this figure. First, the cases for fixed average degree defined level-sets along the diagonal from the lower-left to the higher-right side of the scatterplot. As all cases for $\langle k \rangle = 4 and 6$, irrespectively of the network size N, fall within the rectangle from the origin up to the critical point $(1, 1)$, such configurations are unlikely to produce avalanches. The networks with $\langle k \rangle = 8$ present a transient behavior, being near the transition of the critical region, so that avalanches are expected to be sporadically verified for such an average degree, especially for $N = 50$. All other configurations are likely to exhibit avalanches. The cases for $\langle k \rangle = 12$ are expected to imply particularly sharp avalanches. The configurations with $N = 50$ and $\langle k \rangle = 10$ and 12, as well as $N = 500$ and $\langle k \rangle = 12$, yielded the highest products $r1r2$. Interestingly, no clear order of the values of N can be observed along the level-sets. Recall that the properties of the avalanches will be determined not only by the activation ratios obtained for the most critical level (i.e. that with the largest number of nodes) as in the above discussion, but must also consider the ratios at other levels with significant number of nodes.

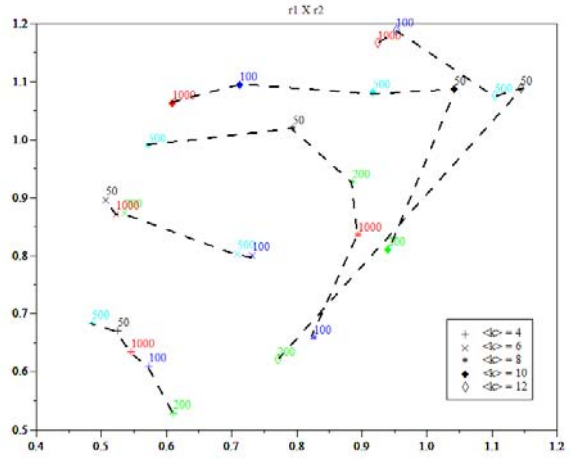

FIG. 5: The scatterplot of $r1 \times r2$ for the most critical level obtained for several configurations of PI networks yielded by the analytical model of the concentric organization reported in this article. The numbers above each point, as well as the respective colors, indicate the network sizes.

TABLE I: The activation ratios for the PI network with $N = 50$, $\langle k \rangle = 4$ and $T = 0.5$.

h	0	1	2	3	4	5
$r1$	0	0.57	0.72	1.05	1.27	1.18
$r2$	0	2.06	1.50	1.35	0.86	0.36
n_h	1	4	10	17	4	1

Figure 6 shows the scatterplot of $r1 \times r2$ for the level with the largest number of nodes obtained for 200 realizations of configurations defined by $\langle k \rangle = 46810$ and 12 and $N = 50$ by considering the whole original networks. As expected, we now have clouds of points instead of the averages produced by the analytical models. Indeed, observe that the analytical averages in Figure 5 tend to appear near the middle of the corresponding clouds in Figure 6. Interestingly, the case for $\langle k \rangle = 6$ exhibits a split, with a few cases appearing near $(r1 = 1.3, r2 = 0.65)$.

Figures 7 to 9 illustrate the spiking dynamics obtained in complete PI networks with $N = 50$ and $\langle k \rangle = 4, 8$ and 12, with the activation source places at the neuron number 1 and $T = 0.5$. More specifically, each of these figures include the spikegram (a) showing the spikes for each neuron along time, and the total number of spikes (b) along time.

The case $N = 50$ and $\langle k \rangle = 4$ shown in Figure 7 yielded the following ratios $r1$ and $r2$ and hierarchical number of nodes n_h for all its 6 concentric levels:

We concentrate attention on the concentric levels 2 and 3, which have the largest number of nodes. Because the respective rations $r1$ and $r2$ are higher or close to 1, it is expected that this configuration will yield a well-defined

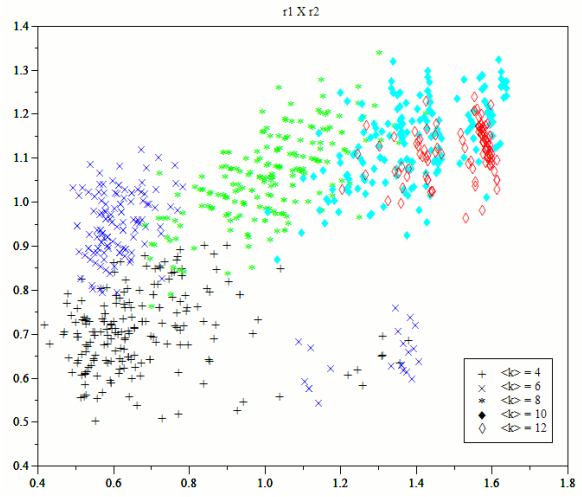

FIG. 6: The scatterplot of $r1 \times r2$ obtained for the concentric level with the largest number of nodes for $N = 50$ and several average degrees considering the whole original PI networks.

avalanche, which is confirmed by the spikegram and total number of spikes along time shown in Figure 7.

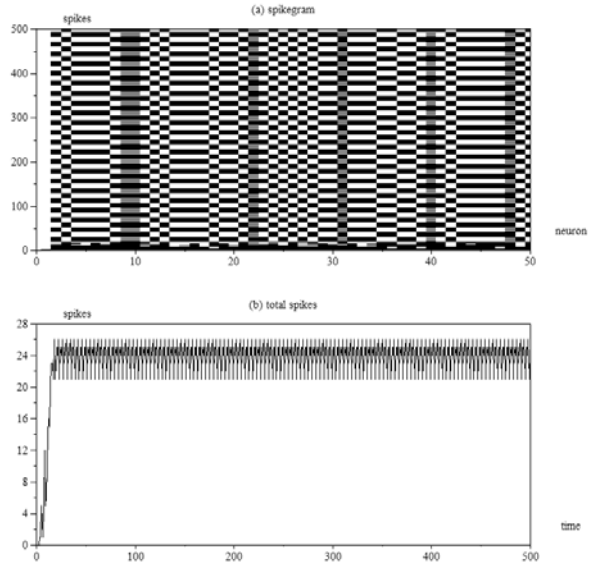

FIG. 7: The spiking dynamics, illustrated in terms of the spikegram (a) and total number of spikes along time (b) for a PI configuration with $N = 50$ and $\langle k \rangle = 4$. $T = 0.5$.

The PI configuration for $N = 50$ and $\langle k \rangle = 8$, implied the following ratios:

Two of the ratios for the levels with the highest number of nodes, namely 1 to 3, are substantially smaller than 1 (0.43 and 0.59), which suggest a weaker avalanche.

TABLE II: The activation ratios for the PI network with $N = 50$, $\langle k \rangle = 8$, and $T = 0.5$.

h	0	1	2	3	4
$r1$	0	0.43	1.59	1.11	1.54
$r2$	0	2.15	2.04	0.59	0.01
n_h	1	8	29	11	1

TABLE III: The activation ratios for the PI network with $N = 50$, $\langle k \rangle = 12$, and $T = 0.5$.

h	0	1	2	3
$r1$	0	0.53	2.29	0.63
$r2$	0	2.25	2.17	0.08
n_h	1	12	35	2

This is confirmed in Figure 8, which shows an avalanche characterized by a relatively gradual transition along the transient regime, followed by saw oscillations (see [13]).

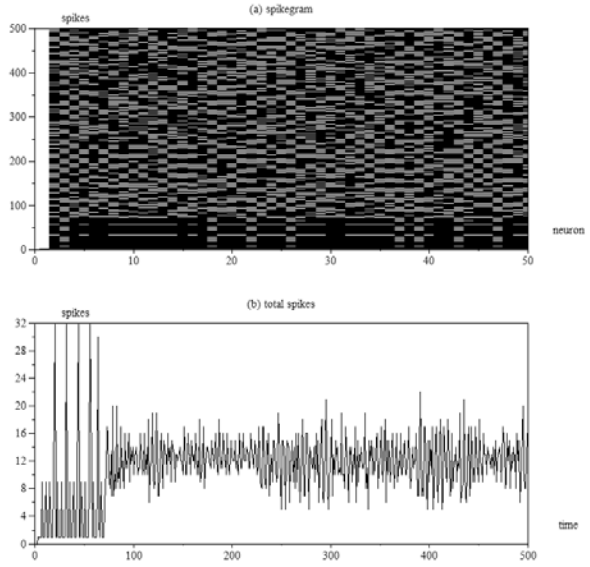

FIG. 8: The spiking dynamics, illustrated in terms of the spikegram (a) and total number of spikes along time (b) for a PI configuration with $N = 50$ and $\langle k \rangle = 8$. $T = 0.5$.

The configuration for $\langle k \rangle = 12$ was characterized by the following ratios:

Again, the two most significant levels (i.e. 1 and 2, containing respectively 12 and 35 nodes), implied one ratio $r1$ substantially smaller than 1, predicting a loose avalanche. Figure 9 shows this to be indeed the case.

The three examples above corroborate the effectiveness of the analytical model for predicting the properties of important dynamical phenomena such as the avalanches of spikes.

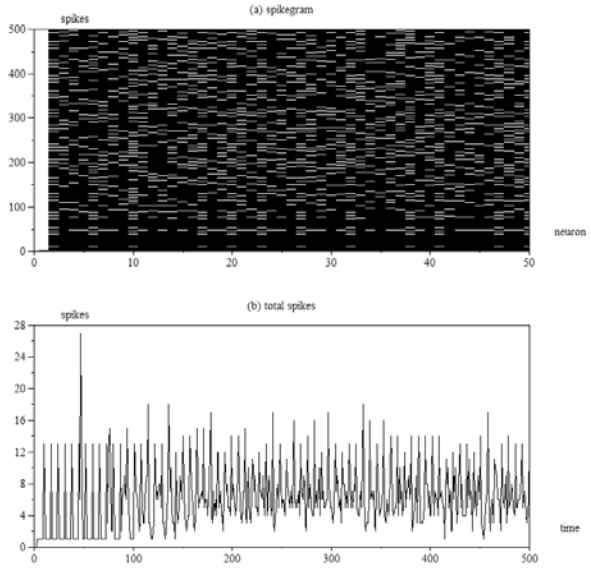

FIG. 9: The spiking dynamics, illustrated in terms of the spikegram (a) and total number of spikes along time (b) for a PI configuration with $N = 50$ and $\langle k \rangle = 12$. $T = 0.5$.

We now turn our attention to the orthogonal lattice complex neuronal networks. Figure 10 shows the scatterplot of $r1 \times r2$ for the level with the largest number of nodes obtained for sizes $N = 50, 100, 200, 500$ and 1000.

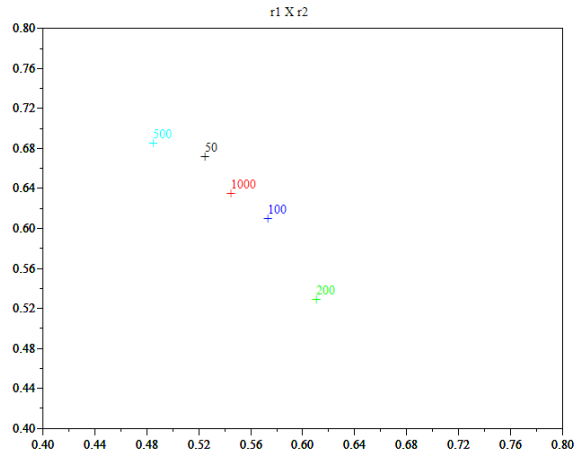

FIG. 10: The scatterplot of $r1 \times r2$ for the level with the largest number of nodes obtained for the orthogonal lattice networks. All cases fall outside the critical region defined by $r1 > 1$ and $r2 > 1$.

Because all the respective points fall well outside the critical region (i.e. $r1 > 1$ and $r2 > 1$), relatively weak avalanches are expected in orthogonal lattice complex neuronal networks. A more complete prediction of the intensity and sharpness of the avalanches needs to consider the activation ratios for other levels associated with many original nodes.

h	0	1	2	3	4	5	6
$r1$	0	0.75	0.83	1.04	1.09	1.14	1
$r2$	0	2	1.5	1.30	1.09	0.76	0.67
n_h	1	4	8	12	12	8	4

h	0	1	2	3	4	5	6	7	8	9	10
$r1$	0	0.75	0.83	0.88	1	1.25	1.17	1.25	1.50	2	1
$r2$	0	2	1.50	1.25	1.17	1.13	1	0.88	0.83	0.75	0.5
n_h	1	4	8	12	16	18	16	12	8	4	1

The configuration for $N = 49$ and $T = 0.5$ yielded the following ratios:

The levels from 2 to 5 are the most critical ones. Except for $r1$ obtained for $h = 2$ (i.e. 0.73) and $r2$ obtained for $h = 5$, all the other ratios are larger than 1, suggesting a well defined avalanche. Figure 11 depicts the spikegram and total spikes along time obtained for this configurations, which confirms the respective prediction.

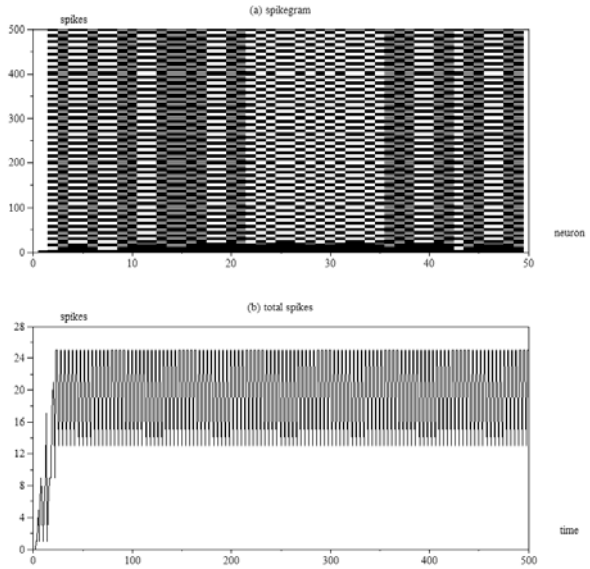

FIG. 11: The spiking dynamics, illustrated in terms of the spikegram (a) and total number of spikes along time (b) for the lattice configuration with $N = 49$. $T = 0.5$.

The ortogonal lattices with N larger than 50 yielded particularly interesting dynamics characterized by lack of clear avalanches, which tended to be replaced by oscillations with increasing frequencies. We illustrate such a behavior with respect to the orthogonal lattice with $N = 484$ and $T = 0.5$, which implied the following ratios:

The levels with the largest number of nodes extend from $h = 2$ to $h = 8$, which have high respective activation ratios $r1$ and $r2$. Figure 12 shows the respective spikegram and total number of spikes along time. Interestingly, though most of the activation ratios are larger than 1, the activation of the network proceeds in terms of oscillations with increasing intensity. Simulations with substantially larger number of time steps showed that this lattice configuration is actually undergoing an avalanche, but with a plateu involving intense saw oscillations.

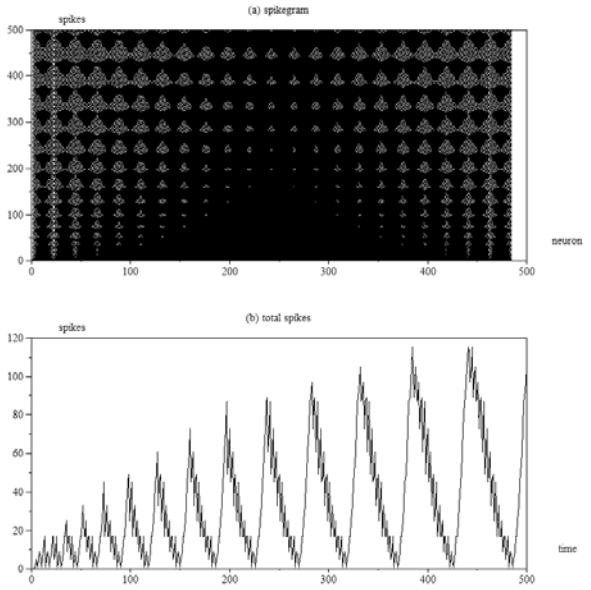

FIG. 12: The spiking dynamics, illustrated in terms of the spikegram (a) and total number of spikes along time (b) for the lattice configuration with $N = 484$. $T = 0.5$.

B. Fixed Action Potential

The dynamics of integrate-and-fire complex neuronal networks with the more biologically-realistic constraint that the action potentials have fixed height implies in a considerably different dynamics of overall activation of the network. The main difference with respect to the case treated in the previous subsection regards the fact that the total internal activation is important only for determining the spiking time, not affecting the intensity of the activation being conveyed to the adjacent concentric levels. That is so because every axon will convey the fixed quantity 1, so that the activation from one level to the next or previous ones depends only on the respective hierarchical degrees, and not on the stored activation.

In this case, the likeliness and intensity (height and sharpness) of the avalanches are related to the following ratios

TABLE IV: The activation ratios for the PI network with $N = 50$, $\langle k \rangle = 4$, $T = 5$.

h	0	1	2	3	4	5	6
$s1$	0	0.22	0.27	0.35	0.40	0.38	0.38
$s2$	0	0.02	0.06	0.13	0.17	0.17	0.19
$s3$	0	0.80	0.55	0.45	0.27	0.12	0.07
n_h	1	4	10	17	13	4	1

TABLE V: The activation ratios for the PI network with $N = 50$, $\langle k \rangle = 12$, $T = 5$.

h	0	1	2	3
$s1$	0	0.57	1.75	0.65
$s2$	0	0.27	0.87	0.33
$s3$	0	2.4	1.66	0.09
n_h	1	12	35	2

$$s1(i) = \frac{k_h(i)}{n_{h+1}(i)} \frac{1}{T}$$
$$s2(i) = \frac{a_h(i)}{n_h(i)} \frac{1}{T}$$
$$s3(i) = \frac{k_h(i-1)}{n_{h-1}(i)} \frac{1}{T}$$

where h is any of the concentric levels with significant number of nodes. Ratio $s1(i)$ quantifies the activation of level h onto the next level $h+1$, $s2(i)$ quantifies the activation of level h over itself, and $s3(i)$ expresses the activation of level h onto the previous level $h-1$. In case any of these ratios are larger than 1, it means that the activation will necessarily imply the firing of the level receiving the activation. The activation rate $s2$ is not particularly important in systems with few concentric levels, provided the critical levels transfers effectively its activation to the adjacent levels. All in all, strong avalanches are expected whenever all or a substantial number of the levels, especially those associated to larger number of original nodes, have the three ratios larger or near 1.

The PI configuration $N = 50$, $\langle k \rangle = 4$ and $T = 5$ yielded:

The levels which are most influent on avalanche formation are levels 2, 3 and 4, which contain 10, 17 and 13 nodes, respectively. Because the three activation ratios, especially $s1$, are much smaller than 1, the activation is expected to be transferred in a more gradual way, which is confirmed by the respective spikegram and total number of spikes in terms of time shown in Figure **??**.

The PI configuration with $N = 50$, $\langle k \rangle = 12$ and $T = 5$ implied the following activation ratios:

The most critical level is $h = 2$, with 35 associated nodes. Because the three activation ratios are either larger or close to 1, a well-defined avalanche would be expected were not for the relatively small values obtained

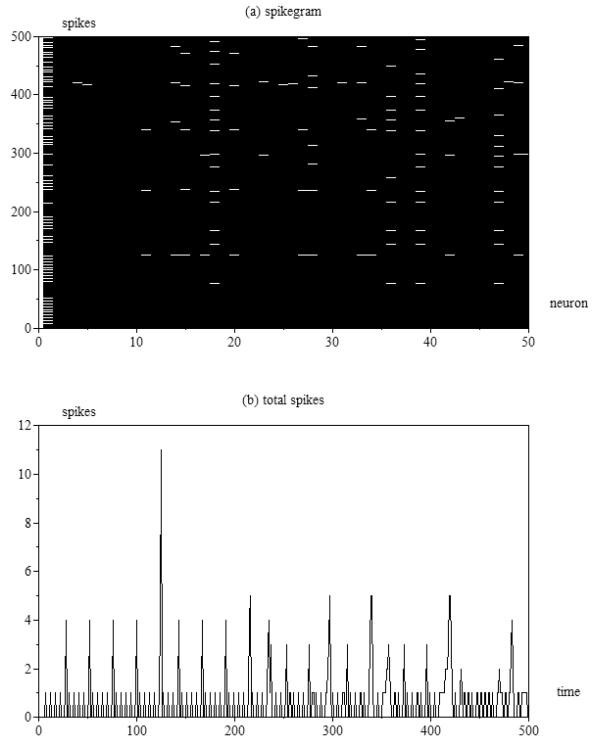

FIG. 13: The spiking dynamics, illustrated in terms of the spikegram (a) and total number of spikes along time (b) for the PI configuration with $N = 50$ and $\langle k \rangle = 4$. $T = 5$.

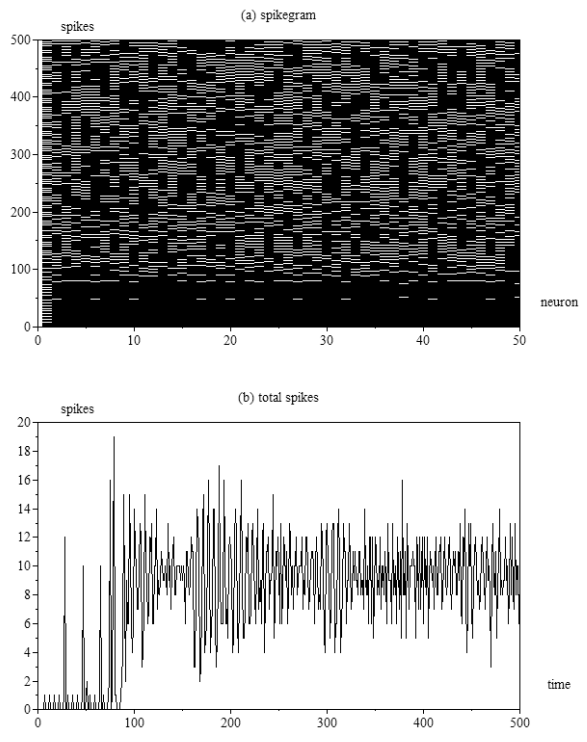

FIG. 14: The spiking dynamics, illustrated in terms of the spikegram (a) and total number of spikes along time (b) for the PI configuration with $N = 50$ and $\langle k \rangle = 12$. $T = 5$.

for $h = 1$. Figure 14 shows the respective spikegram and total number of spikes along time, which confirms the onset of an avalanche at nearly $t = 100$, followed by saw oscillations related to the small activation ratios obtained for $h = 1$.

VII. CONCLUDING REMARKS

Most natural systems can be understood as being underlain by a close relationship between their structure and respective dynamics. Because complex dynamical systems are often characterized by intricate structure *and* dynamics, it becomes critical to devise effective means for characterizing and modeling both these intrinsic components.

The current article has reported the development of analytical models of the node-based concentric organization of orthogonal lattices and path-regular networks, which provide a comprehensive characterization of the topology of the connectivity in these two types of networks. Because of the deterministic nature of the connectivity of orthogonal lattices, exact analytical models of their respective concentric organization could be obtained. On the other hand, because of the stochastic nature of the connectivity in PI networks, a recursive mean field model was developed instead. Both models have been shown to be able to provide highly accurate predictions of the respective hierarchical number of nodes, hierarchical degrees, and intra-ring degrees. The potential of such analytical results has been illustrated with respect to the investigation of avalanches in integrate-and-fire complex neuronal networks underlain by orthogonal lattice and PI connectivity with respect to two types of action potentials (i.e. activation carried by the axons).

The main contributions of this work are listed in the following:

Development of analytical models of concentric organization of orthogonal lattices networks: Though rarely considered in complex networks investigations, orthogonal lattices are particularly interesting because they have deterministic connectivity and perfectly identical node degrees. In this article we developed an exact analytical model of the concentric organization of orthogonal lattices, allowing the calculation of the respective hierarchical number of nodes, hierarchical degrees and intra-ring degrees.

Development of analytical models of concentric organization of PI networks: The family of knitted networks was recently introduced [19, 20] in order to account for the possibility to defined theoreti-

cal models of connectivity founded on path, rather than star-connectivity. This family of networks include the path-transformed BA networks (PA) as well as the path-regular networks (PN). The latter model, which can be obtained by performing several path-walks encompassing all network nodes, has been modified [13] more recently in order to allow identical node degrees. The PN and PI network models are particularly relevant because of the strong regularity regarding measurements taken at distinct nodes or distinct networks. In the current article we developed a mean field analytical model of the PI network, which allows accurate estimations of the concentric organization of the original networks in terms of their hierarchical number of nodes, hierarchical degrees and intra-ring degrees.

Application for structure-function investigations: Because several important features of the dynamics unfolding in complex networks can be estimated from their respective concentric organization (e.g. [13, 14]), more specifically their respective *equivalent models*, the development of analytical models of the concentric features of the orthogonal lattice and path-regular networks has paved the way for comprehensive and systematic investigations of both the structure and dynamics of such networks.

Investigation of Avalanches: In order to illustrate the potential of the analytical models developed in this work, we applied then to characterize and predict the dynamics of avalanches in orthogonal lattice and path-regular complex neuronal networks with integrate-and-fire dynamics. More specifically, the activation ratios were obtained for several configurations (i.e. size and average degree) of these networks. A rich phase space $r1 \times r2$ was obtained for the case of the PI networks, characterized by level-sets of ratios with respect to their average degree. While PI networks with relatively small average degree were found not to produce avalanches, the configurations with lower average degrees implied sharper and stronger avalanches. Such predictions have been corroborated through experimental simulations considering the whole networks. Interestingly, the orthogonal lattice networks yielded small activation ratios, implying weak avalanches.

Consideration of fixed action potential integrate-and-fire dynamics: In this work we considered the integrate-and-fire dynamics with two types of action potentials: distributed and fixes. The former case, adopted in [13, 15], involves distributing the spiking activation (fixed value 1) between the outgoing axons. In the fixed action potentials, each axon had its activation intensity fixed to 1, representing a more biologically-realistic dynamics. The obtained results confirmed preliminary investigations that avalanches are also obtained for fixed action potentials.

The importance of the developments reported in this article can also be substantiated by the following several possibilities for further investigations which have been respectively allowed:

Extension to other types of networks: It would be particularly interesting to extend the analytical models to include other types of networks such as Erdős-Rény, Barabási-Albert, and geographical (e.g. [1–5]). Such models will need to take into account the intrinsic variability of node degree implied by such networks. Yet, the orthogonal lattice and PI models can be used as a comparison reference for other models. For instance, geographical networks are expected to exhibit structural and dynamical properties similar to those of the orthogonal lattice networks.

Extension to other types of dynamics: We have shown that the analytical models, allied with the respective equivalent models, can effectively predict several qualitative and quantitative aspects of non-linear dynamics such as the integrate-and-fire activation. It remains an interesting prospect to investigate how other types of dynamics, such as linear and non-linear diffusion and synchronization, can be modeled and predicted by using the concentric models.

Acknowledgments

Luciano da F. Costa thanks CNPq (308231/03-1) and FAPESP (05/00587-5) for sponsorship.

[1] R. Albert and A. L. Barabási, Rev. Mod. Phys. **74**, 47 (2002).
[2] S. N. Dorogovtsev and J. F. F. Mendes, Advs. in Phys. **51**, 1079 (2002).
[3] M. E. J. Newman, SIAM Rev. **45**, 167 (2003).
[4] S. Boccaletti, V. Latora, Y. Moreno, M. Chavez, and D. Hwang, Phys. Rep. **424**, 175 (2006).
[5] L. da F. Costa, F. A. Rodrigues, G. Travieso, and P. R. V. Boas, Advs. in Phys. **56**, 167 (2007).
[6] L. da F. Costa, M. Kaiser, and C. Hilgetag (2006), arXiv/physics:0607272.
[7] R. Diestel, *Graph Theory* (Springer, 2000).
[8] D. B. West, *Introduction to Graph Theory* (Prentice Hall, 2001).
[9] L. da F. Costa, Phys. Rev. Lett. **93**, 098702 (2004).
[10] L. da F. Costa and R. F. S. Andrade, New J. Phys. **9**, 311 (2007).
[11] L. da F. Costa and F. N. Silva, Journal of Statistical Physics **125**, 845 (2006).
[12] L. da F. Costa and L. E. C. da Rocha, The Eur. Phys. J. B **50**, 237 (2005).
[13] L. da F. Costa (2008), arXiv:0802.0421.
[14] L. da F. Costa (2008), arXiv:0802.1272.
[15] L. da F. Costa (2008), arXiv:0801.3056.

[16] C. Koch, *Biophysics of Computation* (Oxford, 1998).
[17] L. R. Squire, F. E. Bloom, S. K. McConnell, J. L. Roberts, N. S. Spitzer, and M. J. Zigmond, *Fundamental Neuroscience* (Academic Press, 2003).
[18] M. Kaiser, M. Goerner, and C. C. Hilgetag, New J. Phys. **9**, 110 (2007), arXiv:0802.2508.
[19] L. da F. Costa (2007), arXiv:0711.1271.
[20] L. da F. Costa (2007), arXiv:0711.2736.
[21] L. da F. Costa (2007), arXiv:0712.0415.
[22] L. da F. Costa (2008), arXiv:0801.1982.
[23] L. da F. Costa (2008), arXiv:0801.4269.
[24] L. da F. Costa (2008), arXiv:0801.4684.